J. Magn. Soc. Jpn., **41**, 127-131 (2017)

<Paper>

# Synthesis and Magnetic Properties of ($Zn^{2+}Ti^{4+}$) Substituted W-type and Y-type Ferrites

K. Watanabe, K. Kakizaki, and K. Kamishima

Graduate School of Science and Engineering, Saitama University, *255 Shimo-Okubo, Sakura-ku, Saitama 338-8570, Japan*

We report the synthesis of ($Zn^{2+}Ti^{4+}$) substituted hexagonal ferrites, $BaZn_2(Zn_{0.5}Ti_{0.5})_xFe_{16-x}O_{27}$ (W-type) and $Ba_2Zn_2(Zn_{0.5}Ti_{0.5})_xFe_{12-x}O_{22}$ (Y-type), and the relationship between their composition and magnetic properties. Substituted W-type ferrite was synthesized in the region of $0.0 \leq x \leq 1.5$. A decrease in the Curie temperature of the W-type phase indicated that the exchange interactions between the $Fe^{3+}$ ions weakened due to the substitution of $Zn^{2+}$ and $Ti^{4+}$ ions. Spontaneous magnetization ($\sigma_S$) at $x = 0.5$ was similar to that at $x = 0.0$. This reflects the equal distribution of nonmagnetic $Zn^{2+}$ and $Ti^{4+}$ ions to spin down sites and spin up sites, respectively. At $x > 0.5$, $\sigma_S$ decreased clearly, which was possibly caused by a deviation from the collinear arrangement. Substituted Y-type ferrite was also obtained up to $x = 0.5$. The Y-type phase is more unstable than the W-type phase with respect to this substitution rate.

**Key words:** W-type ferrite, Y-type ferrite, (ZnTi) substitution, solid state reaction, X-ray diffraction, Curie temperature, spontaneous magnetization, cation distribution

## 1. Introduction

The hexagonal ferrites have been investigated for electronic devices at microwave frequencies since their discovery in 1950s [1]. Their availability at high frequencies is caused by the large magnetic anisotropy constants and the preference to several magnetized directions, parallel or perpendicular to the hexagonal *c*-axis. Most of ferrites also have low eddy current loss at high frequency and corrosive resistance because they are oxides.

The crystal structure of hexagonal ferrites is based upon the close-packed structure of large oxygen anions and barium cations. The small transition metal cations ($Fe^{3+}$ and $Me^{2+}$) are located between the larger ions. The structures of hexagonal ferrites can be represented by the stacking combinations along their hexagonal *c*-axis of R, S, and T blocks [2]. The chemical formulae for these blocks are as follows: R = $(BaFe_6O_{11})^{2-}$, S = $Me_2Fe_4O_8$ / $(Fe_6O_8)^{2+}$, T = $Ba_2Fe_8O_{14}$. The composition of the S block corresponds with the two formula units of the spinel ferrite. The major hexagonal ferrites are described by the following symbols: $RSR^*S^*$ for M-type ($BaFe_{12}O_{19}$), $(RSR^*S^*S^*)_3$ for X-type ($Ba_2Me_2Fe_{28}O_{46}$), $RSSR^*S^*S^*$ for W-type ($BaMe_2Fe_{16}O_{27}$), $(TS)_3$ for Y-type ($Ba_2Me_2Fe_{12}O_{22}$), $RSTSR^*S^*T^*S^*$ for Z-type ($Ba_3Me_2Fe_{24}O_{41}$), and $(RSTSR^*S^*)_3$ for U-type ($Ba_4Me_2Fe_{36}O_{60}$) [3, 4]. The superscript * denotes that the layer is turned for 180° around the *c*-axis.

M-type barium ferrite ($BaFe_{12}O_{19}$) is widely used for permanent magnets due to its large magneto-crystalline anisotropy [5]. In addition, many research groups have investigated barium ferrite as microwave absorbers [6-8] and magnetic recording media [9] by modifying its anisotropy. The control of its magnetic property is achieved by the replacement of $Fe^{3+}$ ions by $Al^{3+}$ [10-13], $Cr^{3+}$ [13-15] ions or pairs of ($Me^{2+}Mt^{4+}$) ions such as ($Co^{2+}Ti^{4+}$) [16, 17], ($Zn^{2+}Ti^{4+}$) [18, 19], ($Mn^{2+}Ti^{4+}$) [6, 20], ($Ni^{2+}Sn^{4+}$) [21], ($Co^{2+}Sn^{4+}$) [22], ($Co^{2+}Zr^{4+}$) [23, 24], where the Me and Mt represent divalent and tetravalent cations, respectively. The substitution effect on anisotropy is so significant that even the hard magnetic property of $BaFe_{12}O_{19}$ was changed to soft magnetic by substitution of $(Co^{2+}Zn^{2+})Ti^{4+}$ for $Fe^{3+}$ [25].

On the other hand, W-type and Y-type ferrites have different magnetic properties from those of M-type ferrite due to their different stacking structures. W-type ferrite can possess higher saturation magnetization than that of M-type ferrite [26]. Y-type ferrite has planar anisotropy [27], which gives hope for high-frequency application. Therefore, the control of the magnetic properties of W-type and Y-type ferrites has been an important issue.

To the best of our knowledge, however, there are few investigations on the substituted W-type and Y-type ferrite. Maeda *et al.* reported the preparation by a conventional ceramic technique, magnetic properties, and microwave absorption properties of the ($Mn^{2+}Sn^{4+}$) and ($Mn^{2+}Zr^{4+}$) substituted W-type ferrite [28]. Ul-ain *et al.* reported the synthesis by sol-gel method and catalytic activities of the ($Mn^{2+}Ti^{4+}$) substituted Y-type ferrite [29]. Also, substitution limits of $Me^{2+}Mt^{4+}$ for $Fe^{3+}$ in W-type and Y-type structures are unclear in contrast with that in the M-type structure where complete substitution of $Co^{2+}Ti^{4+}$ for $Fe^{3+}$ is possible to form $BaCo_6Ti_6O_{19}$ [30].

We report the synthesis of the ($Zn^{2+}Ti^{4+}$) substituted hexagonal ferrites, $BaZn_2(Zn_{0.5}Ti_{0.5})_xFe_{16-x}O_{27}$ (W-type) and $Ba_2Zn_2(Zn_{0.5}Ti_{0.5})_xFe_{12-x}O_{22}$ (Y-type), and the relation between their composition and magnetic properties in this paper. Here, we employed $Zn^{2+}Ti^{4+}$ cations for substitution because an increase of the magnetization was expected if nonmagnetic cations replaced Fe cations

in spin down sublattices as observed in substituted spinels [31].

## 2. Experimental procedure

The samples were prepared by solid-state reaction. We used $BaCO_3$, ZnO, $TiO_2$, and $\alpha$-$Fe_2O_3$ as starting materials. They were mixed in the desired composition of Ba : Zn : $(Zn_{0.5}Ti_{0.5})$ : Fe = 1 : 2 : $x$ : (16-$x$) for the W-type ferrite and Ba : Zn : $(Zn_{0.5}Ti_{0.5})$ : Fe = 2 : 2 : $x$ : (12-$x$) for the Y-type ferrite with $0.0 \leq x \leq 2.0$ in a ball-milling pot for 24 h. The mixed powders were pressed into disks and then pre-sintered at 900°C in air for 5 h. The products were ground in a mortar and then pulverized for 10 min. at the rate of 1100 r.p.m. in a vario-planetary mill. The fine powders were pressed into disks again and then sintered at 1100-1350°C in air for 5 h. Finally, the products were ground into powders in a mortar.

The crystal structures were examined by powder X-ray diffraction (XRD) with Cu-Kα radiation. The magnetizations were measured with a vibrating sample magnetometer (VSM), and a superconducting quantum interference device magnetometer (SQUID).

## 3. Results and discussion

We identified the crystalline phases of the W-type composition samples with $0.0 \leq x \leq 2.0$ sintered at 1200-1350°C by XRD. Fig. 1 shows phase relationship between sintering temperature and substitution rate $x$. At $0.0 \leq x \leq 1.5$, the W-type phase formed in the samples sintered at 1250°C, provided that the W-type phase was the minority phase for the sample with $x$ = 1.5. The samples with $0.0 \leq x \leq 1.5$ sintered at 1300°C and 1350°C consisted of the main W-type phase. On the other hand, at sintering temperature of 1350°C, the sample contained the M-type and spinel minority phases. Since this temperature is near to the melting point of the other barium-iron oxides (e. g. $Ba_2Fe_2O_5$; $T_m$ = 1370°C [32]), the W-type phase is likely to decompose. These results show that the sintering temperature of 1300°C is the suitable condition for the synthesis of the substituted W-type ferrites.

Fig. 2 shows XRD patterns of W-type composition samples with Ba : Zn : $(Zn_{0.5}Ti_{0.5})$ : Fe = 1 : 2 : $x$ : (16-$x$) sintered at 1300°C. The samples had the W-type structure at $0.0 \leq x \leq 1.5$. At $x$ = 1.5, there were some

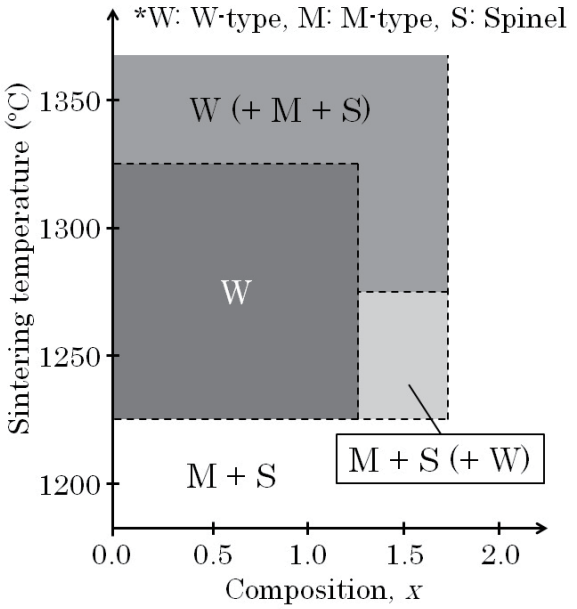


**Fig. 1** Relationship between obtained crystalline phase and sintering temperature and substitution rate $x$ for samples whose raw materials were mixed in composition of Ba : Zn : $(Zn_{0.5}Ti_{0.5})$ : Fe = 1 : 2 : $x$ : (16-$x$) with $0.0 \leq x \leq 2.0$. Phases in parentheses are minority phases.

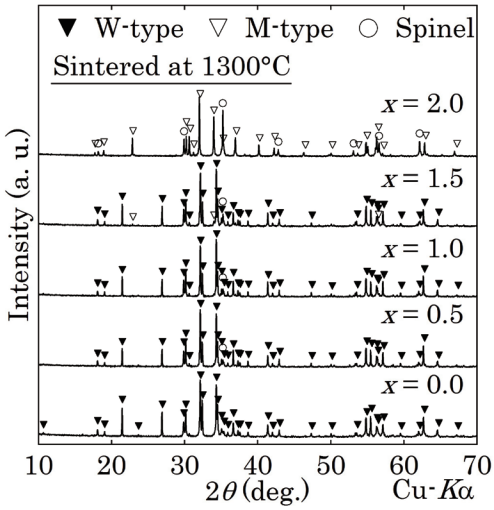


**Fig. 2** XRD patterns for products sintered at 1300°C whose raw materials were mixed in composition of Ba : Zn : $(Zn_{0.5}Ti_{0.5})$ : Fe = 1 : 2 : $x$ : (16-$x$) with $0.0 \leq x \leq 2.0$.

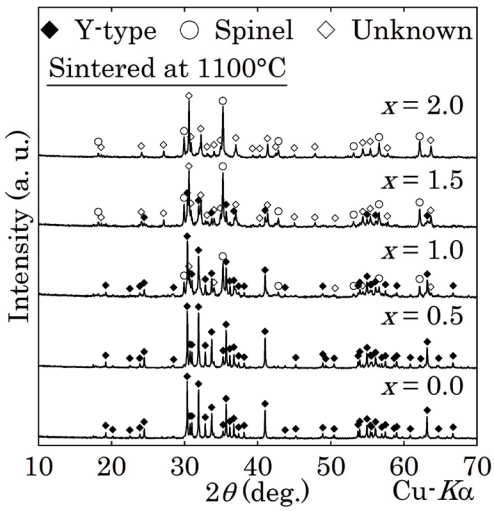


**Fig. 3** XRD patterns for products sintered at 1100°C whose raw materials were mixed in composition of Ba : Zn : $(Zn_{0.5}Ti_{0.5})$ : Fe = 2 : 2 : $x$ : (12-$x$) with $0.0 \leq x \leq 2.0$.

weak diffraction peaks of the M-type and spinel ferrites. On the contrary, the peaks of the W-type phase disappeared in the pattern at $x = 2.0$. It should be noted that the first and second peaks of the W-type phase do not overlap those of the spinel and M-type phases as comparing the patterns between $x \leq 1.5$ and $x = 2.0$. Fig. 3 shows XRD patterns of Y-type composition samples with Ba : Zn : $(Zn_{0.5}Ti_{0.5})$ : Fe = 2 : 2 : $x$ : (12-$x$) sintered at 1100°C. We obtained the Y-type phase in the samples with $x = 0.0$ and 0.5. On the other hand, the diffraction peaks of the Y-type phase weakened at $x \geq 1.0$ and finally disappeared at $x = 2.0$. The phase identification was based on the diagrams of the $BaO$-$ZnO$-$Fe_2O_3$ [33], $BaO$-$ZnO$-$TiO_2$ [34] and $BaO$-$Fe_2O_3$-$TiO_2$ [35] systems, which showed no corresponding compounds except for the spinel and Y-type phases. The maximum substitution rate of (ZnTi)/(Fe+(ZnTi)) to form the single Y-type phase (0.5/12 ~ 4.2%) is smaller than that to form the single W-type phase (1.0/16 ~ 6.3%). Therefore, the Y-type phase is less stable than the W-type phase for $(Zn^{2+}Ti^{4+})$ substitution.

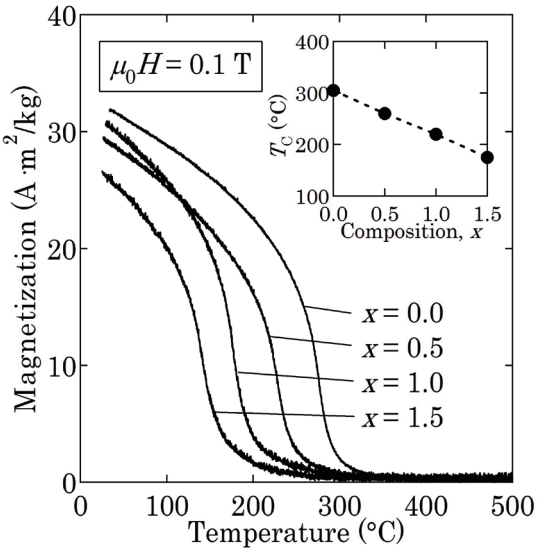


**Fig. 4** Temperature dependences of magnetization at $\mu_0H = 0.1$ T for samples sintered at 1300°C whose raw materials were mixed in composition of $BaZn_2(Zn_{0.5}Ti_{0.5})_xFe_{16-x}O_{27}$ with $0.0 \leq x \leq 1.5$. Inset shows Curie temperatures $T_C$ of those samples.

Fig. 4 shows temperature dependences of magnetization at $\mu_0H = 0.1$ T for W-type composition samples of $BaZn_2(Zn_{0.5}Ti_{0.5})_xFe_{16-x}O_{27}$ ($0.0 \leq x \leq 1.5$) sintered at 1300°C. Inset of Fig. 4 shows the Curie temperature $T_C$ of the W-type phase as a function of the composition $x$, where $T_C$ was estimated by linear extrapolation to zero-magnetization from the inflection point of the $M$-$T$ curve. The Curie temperature $T_C$ of the no-substitution sample ($x = 0.0$) was 305°C, which is in agreement with the previous report about $BaZn_2Fe_{16}O_{27}$ single crystals [36]. $T_C$ linearly decreased with increasing $x$ at $x \leq 1.5$, suggesting the exchange interactions between $Fe^{3+}$ ions weakened. This fact implies that $Zn^{2+}$ and $Ti^{4+}$ cations successfully replaced $Fe^{3+}$ cations in the W-type structure at $x \leq 1.5$.

Fig. 5 shows magnetization curves at $T = 5$ K (= –268°C) for W-type samples of $BaZn_2(Zn_{0.5}Ti_{0.5})_xFe_{16-x}O_{27}$ ($0.0 \leq x \leq 1.5$) sintered at 1300°C. The magnetization curve of the substituted samples at $x = 0.5$ was almost the same as that of the no-substitution sample ($x = 0.0$). Then, the magnetization decreased with increasing the substitution rate from $x = 0.5$ up to 1.5. This result is consistent with the fact that M-type ferrite showed similar Zn-Ti substitution dependence of spontaneous magnetization [37], where the magnetization began to

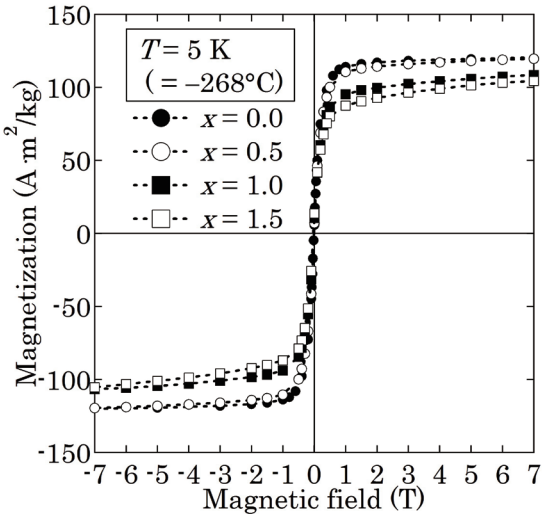


**Fig. 5** Magnetization curves at $T = 5$ K (= –268°C) for samples sintered at 1300°C whose raw materials were mixed in composition of $BaZn_2(Zn_{0.5}Ti_{0.5})_xFe_{16-x}O_{27}$ with $0.0 \leq x \leq 1.5$.

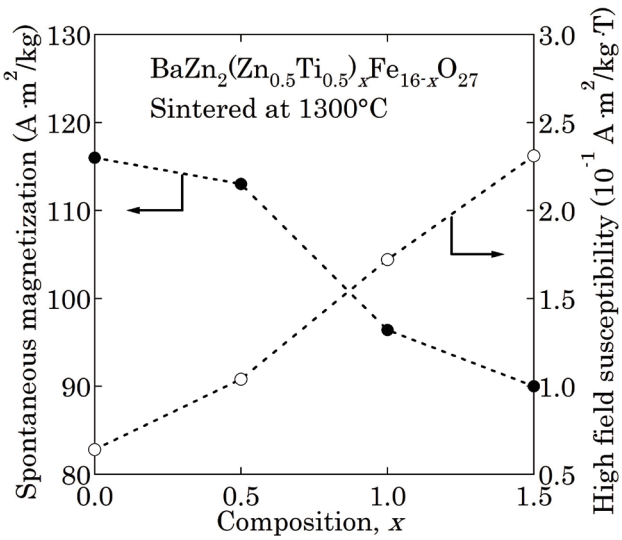


**Fig. 6** Spontaneous magnetization and high field differential susceptibility for samples sintered at 1300°C whose raw materials were mixed in composition of $BaZn_2(Zn_{0.5}Ti_{0.5})_xFe_{16-x}O_{27}$ with $0.0 \leq x \leq 1.5$.

decrease above a certain Zn-Ti substitution rate.

Fig. 6 shows spontaneous magnetization $\sigma_S$ and high field differential susceptibility $\chi_d$ as a function of the composition $x$. They were estimated by linear extrapolation of the magnetization curves from a high field region. The spontaneous magnetization $\sigma_S$ slightly decreased from $x = 0.0$ to 0.5. In the range of $0.5 < x \leq 1.5$, the decrease of $\sigma_S$ became more obvious. The substitution effect on $\sigma_S$ seems to reflect $Zn^{2+}$-$Ti^{4+}$ cation distribution in the W-type structure.

In order to discuss the relationship between the change in $\sigma_S$ and the cation distribution in the W-type structure, we consider the spin configuration of the W-type structure. Table 1 shows the distribution of the transition metal sites and the expected directions of the magnetic moments in the R and S blocks of the W-type structure [38]. Fig. 7 also shows magnetic structure of W-type ferrite, corresponding to Table 1.

Concerning the cation distribution in the W-type structure, we assume that the $Zn^{2+}$ ions prefer the 4*e* and 4$f_{IV}$ sites and that $Ti^{4+}$ ions prefer the 12*k* sites. In the case of the (ZnTi) substituted M-type ferrite [37], $Zn^{2+}$ ions tend to enter the tetrahedral 4$f_{IV}$ sites in the S block. Also, $Ti^{4+}$ ions tend to enter the octahedral 4$f_{VI}$ (the R block) sites and the 12*k* (the S and R blocks border) sites. In our W-type ferrite case, even with no substitution sample of $x = 0.0$, however, the positively charged part of two S blocks of $(Zn_2Fe_{10}O_{16})^{2+}$ and the negatively charged R block of $(BaFe_6O_{11})^{2-}$ are alternately stacked up as SSRS*S*R*. The additional $Zn^{2+}$ ions seem to occupy 4*e* and 4$f_{IV}$ sites in the S blocks like the ZnTi-doped M-type ferrite. In order to keep the local electronic balance in the additional $Zn^{2+}$ doped S blocks, $Ti^{4+}$ ions may prefer the 12*k* sites to the 4$f_{VI}$ sites because of the proximity to the $Zn^{2+}$ sites in the S block.

We discuss the effect of the nonmagnetic ions upon the spontaneous magnetization $\sigma_S$ depending on $x$. Between $x = 0.0$ and 0.5, the occupation of spin down (4*e* and 4$f_{IV}$) sites by $Zn^{2+}$ ions can be cancelled out by the occupation of spin up (12*k*) sites by $Ti^{4+}$ ions. Therefore, the decrease of $\sigma_S$ is slight in this range. At $x > 0.5$, the obvious decrease of $\sigma_S$ is possibly caused by the deviation from the collinear arrangement which can be dominant at high substitution rates of $Zn^{2+}$ and $Ti^{4+}$ ions [37]. To ascertain our estimation, further experimental investigations are needed to estimate the spin configuration and the cation distribution by Rietveld analysis on powder neutron diffraction [39] and X-ray absorption fine structure analysis [40].

The high field differential susceptibility $\chi_d$ for the substituted W-type ferrite increases with increasing $x$ as shown in Fig. 6. It suggests that the magnetic structure of the substituted W-type ferrite becomes non-collinear especially at $x > 0.5$. It is consistent with the interpretation of the variation in $\sigma_S$ discussed above.

**Table 1** Coordination, number of ions, and spin orientation for various cation sublattices of W-type ferrite.

| Block | Sublattice | Coordination | Number per block | Spin |
|---|---|---|---|---|
| S-S | 6*g* | Octahedral | 3 | Up |
| S | 4*e* | Tetrahedral | 2 | Down |
| S | 4*f* | Octahedral | 2 | Up |
| S | 4$f_{IV}$ | Tetrahedral | 2 | Down |
| S-R | 12*k* | Octahedral | 6 | Up |
| R | 4$f_{VI}$ | Octahedral | 2 | Down |
| R | 2*d* | Trigonal -bipyramidal | 1 | Up |

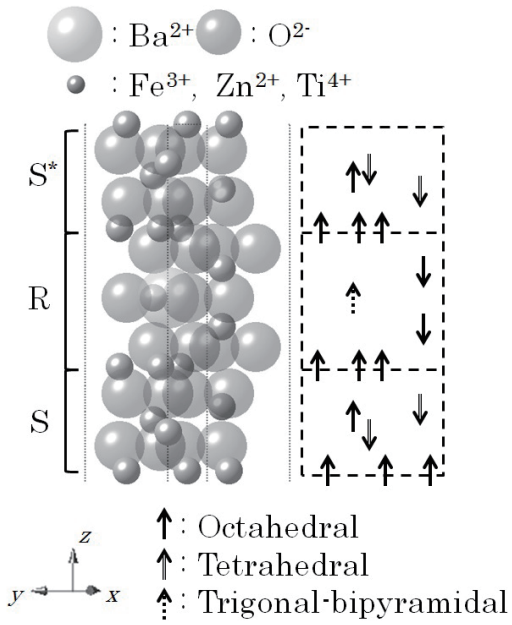


**Fig. 7** Magnetic structure in half of unit cell (in formula unit ) of W-type ferrite.

## 4. Conclusions

We report the synthesis condition and the magnetic properties of the $(Zn^{2+}Ti^{4+})$-substituted W-type and Y-type hexagonal ferrites that have hardly been investigated so far. The synthesis condition shows the substitution limits of $Zn^{2+}Ti^{4+}$ for $Fe^{3+}$ in the W-type and Y-type ferrites, suggesting the stability of the W-type and Y-type structures.

The W-type composition samples sintered at 1300°C had the W-type structure in the region of $0.0 \leq x \leq 1.5$. The Curie temperature of the W-type phase decreased linearly with increasing $x$ at $x \leq 1.5$. It suggests that the exchange interactions between the $Fe^{3+}$ ions weakened due to the substitution of nonmagnetic $Zn^{2+}$ and $Ti^{4+}$ ions in the W-type structure. Spontaneous magnetization $\sigma_S$

at $x = 0.5$ was similar to that at $x = 0.0$. It reflects the equal distribution of nonmagnetic $Zn^{2+}$ and $Ti^{4+}$ ions to spin down sites and spin up sites, respectively. At $x > 0.5$, $\sigma_s$ decreased clearly, which is possibly caused by the deviation from the collinear arrangement. It is consistent with the increase in the high field differential susceptibility $\chi_d$ with $x$.

The Y-type single phase was also obtained for the Y-type composition samples up to $x = 0.5$. The Y-type phase is more unstable than the W-type phase with respect to this substitution rate.

## References


1) G. H. Jonker, H. P. J. Wijn and P. B. Braun: *Philips Tech. Rev.*, **18**, 145, (1956-1957).
2) J. Smit and H. P. Wijn: *Ferrites*, p. 150, 151, 180-189 (Philips Technical Library, London, 1959).
3) P. B. Braun: *Philips Res. Rep.*, **12**, 491-548 (1957).
4) T. Honda, Y. Hiraoka, Y. Wakabayashi and T. Kimura: *J. Phys. Soc. Jpn.*, **82**, 025003 (2013).
5) U. Ozgur, Y. Alivov and H. Morkoc: *J. Mater. Sci: Mater. Electron*, **20**, 789-834 (2009).
6) S. Sugimoto, K. Okayama, S. Kondo, H. Ota, M. Kimura, Y. Yoshida, H. Nakamura, D. Book, T. Kagotani and M. Homma: *Mater. Trans. JIM*, **39**, 1080-1083 (1998).
7) S. Sugimoto, S. Kondo, K. Okayama, H. Nakamura, D. Book, T. Kagotani and M. Homma: *IEEE Trans. Magn.*, **35**, 3154-3156 (1999).
8) K. Haga, S. Sugimoto, T. Kagotani and K. Inomata: *Mater. Trans.*, **45**, 2606-2609 (2004).
9) D. H. Han and Z. Yang: *IEEE Trans. Magn.*, **31**, 2351-2354 (1995).
10) A. V. Trukhanov, N. T. Dang, S. V. Trukhanov, S. H. Jabarov, I. S. Kazakevich, A. I. Mammadov, R. Z. Mekhdiyeva, V. A. Turchenko, and R. E. Huseynov: *Phys. Solid State*, **58**, 992–996 (2016).
11) C. J. Li, B. N. Huang and J. N. Wang: *J. Mater. Sci.*, **48**, 1702-1710 (2013).
12) S. M. El-Sayed, T. M. Meaz, M. A. Amer and H. A. El Shersaby: *Physica B*, **426**, 137-143 (2013).
13) J. Qiu, M. Gu and H. Shen: *J. Magn. Magn. Mat.*, **295**, 263-268 (2005).
14) J. Qiu, Y. Wang and M. Gu: *Mater. Lett.*, **60**, 2728-2732 (2006).
15) T. M. Meaz and C. B. Koch: *Hyperf. Interact*, **166**, 455-463 (2005).
16) A. M. Alsmadi, I. Bsoul, S. H. Mahmood, G. Alnawashi and K. Prokes: *J. Appl. Phys.*, **114**, 243910 (2013).
17) Y. Guan, Y. Lin, L. Zou, Q. Miao, M. Zeng, Z. Liu, X. Gao and J. Liu: *AIP Advances.*, **3**, 122115 (2013).
18) J. Li, H. Zhang, Y. Liu, Q. Li, G. Ma and H. Yang: *J. Mater. Electron,* **26**, 1060-1065 (2015).
19) Z. Yang, C. S. Wang, X. H. Li and H. X. Zeng: *Mater. Sci. Eng.*, **B90**, 142–145 (2002).
20) Y. S. Hong, C. M. Ho, H. Y. Hsu and C. T. Liu: *J. Magn. Magn. Mat.*, **279**, 401-410 (2004).
21) A. Gonzalez-Angelesa, G. Mendoza-Suareza, A. Gruskova, I. Toth, V. Jancarik, M. Papanova and J. I. Escalante-Garcia: *J. Magn. Magn. Mat.*, **270**, 77-83 (2004).
22) X. Gao, Y. Du, X. Liu, P. Xu and X. Han: *Mater. Res. Bull.*, **46**, 643-648 (2011).
23) R. K. Mudsainiyan, S. K. Chawla, S. S. Meena, N. Sharma, R. Singh and A. Das: *Ceram. Int.*, **40**, 16617-16626 (2014).
24) J. Zhou, H. Ma, M. Zhong, G. Xu, Z. Yue and Z. He: *J. Magn. Magn. Mat.*, **305**, 467-469 (2006).
25) K. Miyata, K. Kamishima, K. Kakizaki and N. Hiratsuka: *J. Magn. Soc. Jpn.*, **30**, 383-386 (2006) [in Japanese].
26) S. Chikazumi: Physics of Ferromagnetism, p. 213 (Oxford University Press, Oxford, 2009).
27) Ibid. 26, p. 282.
28) Y. Maeda, T. Kagotani, H. Nakamura, D. Book, S. Sugimoto and M. Homma: *J. Magn. Soc. Jpn.*, **24**, 895-898 (2000) [in Japanese].
29) B. Ul-ain, S. Ahmed, M. Anis ur Rehman, Y. Huang and C. A. Randall: *New J. Chem.*, **37**, 2768-2777 (2013).
30) A. Labarta, X. Batlle, B. Martínez, and X. Obradors: *Phys. Rev. B*, **46**, 8994-9001 (1992).
31) Ibid. 26, p. 204.
32) Y. Goto and T. Takada: *J. Am. Ceram. Soc.*, **43**, 150-153 (1960).
33) C. Slokar and E. Lucchini: *J. Magn. Magn. Mat.*, **8**, 232-236 (1978).
34) Phase Equilibria Diagrams, The American Ceramic Society and the National Institute of Standards and Technology, Figure Number 10032.
35) T. Siegrist and T. A. Vanderah: *Eur. J. Inorg. Chem.*, 1483-1501 (2003).
36) R. O. Savage and A. Tauber: *J. Am. Ceram. Soc.*, **47**, 13 (1964).
37) P. Wartewig, M. K. Krause, P. Esquinazi, S. Rosler and R. Sonntag: *J. Magn. Magn. Mat.*, **192**, 83-99 (1999).
38) G. Albanese and M. Carbucicchio: *Appl. Phys.*, **11**, 81-88 (1976).
39) T. Tachibana, T. Nakagawa, Y. Takada, K. Izumi, T. A. Yamamoto, T. Shimada and S. Kawano: *J. Magn. Magn. Mat.*, **262**, 248-257 (2003).
40) T. Nakagawa, M. Yuya, T. Tachibana, Y. Takada, H. Nitani, S. Emura, T. A. Yamamoto: *J. Magn. Magn. Mat.*, **288**, 366-373 (2005).


**Received Jul. 20, 2017; Revised Sept. 3, 2017; Accepted Sept. 19, 2017**